OXFORD

JNCI J Natl Cancer Inst (2016) 108(11): djw148

doi: 10.1093/jnci/djw148
First published online July 5, 2016
Article

ARTICLE

Mechanisms of Therapy Resistance in Patient-Derived Xenograft Models of BRCA1-Deficient Breast Cancer

Petra ter Brugge, Petra Kristel, Eline van der Burg, Ute Boon, Michiel de Maaker, Esther Lips, Lennart Mulder, Julian de Ruiter, Catia Moutinho, Heidrun Gevensleben, Elisabetta Marangoni, Ian Majewski, Katarzyna Jóźwiak, Wigard Kloosterman, Markus van Roosmalen, Karen Duran, Frans Hogervorst, Nick Turner, Manel Esteller, Edwin Cuppen, Jelle Wesseling, Jos Jonkers

Affiliations of authors: Division of Molecular Pathology and Cancer Genomics Centre Netherlands (PtB, PK, EvdB, UB, MdM, EL, LM, JdR, JW, JJ), Division of Molecular Carcinogenesis (IM), Department of Epidemiology and Biostatistics (KJ), and Family Cancer Clinic and Department of Pathology (FH), The Netherlands Cancer Institute, Amsterdam, the Netherlands; Cancer Epigenetics and Biology Program (PEBC), Bellvitge Biomedical Research Institute (IDIBELL), Barcelona, Catalonia, Spain (CM, ME); The Breakthrough Breast Cancer Research Centre, Institute of Cancer Research, London, UK (HG, NT); Laboratory of Preclinical Investigation, Translational Research Department, Curie Institute, Paris, France (EM); Department of Medical Genetics, University Medical Center Utrecht, Utrecht, the Netherlands (WK, MvR, KD, EC); Department of Physiological Sciences II, School of Medicine, University of Barcelona, Barcelona, Catalonia, Spain (ME); Institucio Catalana de Recerca i Estudis Avançats (ICREA), Barcelona, Catalonia, Spain (ME)

Current affiliation: Institute of Pathology, University Hospital Bonn, Bonn, Germany (HG); The Walter and Eliza Hall Institute of Medical Research, Parkville, VIC, Australia (IM).
Correspondence to: Jos Jonkers, PhD, Division of Molecular Pathology and Cancer genomics Centre Netherlands, The Netherlands Cancer Institute, Plesmanlaan 121, 1066CX Amsterdam, the Netherlands (e-mail: j.jonkers@nki.nl); or Jelle Wesseling, MD, PhD, Division of Molecular Pathology and Cancer genomics Centre Netherlands, The Netherlands Cancer Institute, Plesmanlaan 121, 1066CX Amsterdam, the Netherlands (e-mail: j.wesseling@nki.nl).

Abstract

Background: Although BRCA1-deficient tumors are extremely sensitive to DNA-damaging drugs and poly(ADP-ribose) polymerase (PARP) inhibitors, recurrences do occur and, consequently, resistance to therapy remains a serious clinical problem. To study the underlying mechanisms, we induced therapy resistance in patient-derived xenograft (PDX) models of *BRCA1*-mutated and *BRCA1*-methylated triple-negative breast cancer.
Methods: A cohort of 75 mice carrying BRCA1-deficient breast PDX tumors was treated with cisplatin, melphalan, nimustine, or olaparib, and treatment sensitivity was determined. In tumors that acquired therapy resistance, BRCA1 expression was investigated using quantitative real-time polymerase chain reaction and immunoblotting. Next-generation sequencing, methylation-specific multiplex ligation-dependent probe amplification (MLPA) and Target Locus Amplification (TLA)–based sequencing were used to determine mechanisms of BRCA1 re-expression in therapy-resistant tumors.
Results: BRCA1 protein was not detected in therapy-sensitive tumors but was found in 31 out of 42 resistant cases. Apart from previously described mechanisms involving *BRCA1*-intragenic deletions and loss of *BRCA1* promoter hypermethylation, a novel resistance mechanism was identified in four out of seven *BRCA1*-methylated PDX tumors that re-expressed BRCA1 but retained *BRCA1* promoter hypermethylation. In these tumors, we found de novo gene fusions that placed *BRCA1* under the transcriptional control of a heterologous promoter, resulting in re-expression of BRCA1 and acquisition of therapy resistance.
Conclusions: In addition to previously described clinically relevant resistance mechanisms in *BRCA1*-deficient tumors, we describe a novel resistance mechanism in *BRCA1*-methylated PDX tumors involving de novo rearrangements at the *BRCA1*

Received: December 2, 2015; **Revised:** March 17, 2016; **Accepted:** May 12, 2016

locus, demonstrating that *BRCA1*-methylated breast cancers may acquire therapy resistance via both epigenetic and genetic mechanisms.

Each year around 150 000 million women are diagnosed with triple-negative breast cancer (TNBC) (1). A substantial percentage of TNBCs are homologous recombination (HR)–deficient (HRD) because of BRCA1 pathway inactivation (1–3). BRCA1-deficient cells are sensitive to DNA double-strand break (DSB)–inducing agents, in particular alkylators that induce DNA-crosslinks. Preclinical (4–7) and neoadjuvant studies (8,9) have shown *BRCA1*-mutated tumors and possibly also sporadic TNBCs with low BRCA1 expression (10) to be sensitive to cisplatin monotherapy. Cells with BRCA pathway defects are also extremely sensitive to poly(ADP-ribose) polymerase-1 (PARP1) inhibitors, which indirectly induce DSBs that cannot be efficiently repaired in HRD cells (11–14). Preclinical (5,15,16) and clinical studies (17,18) indeed showed that *BRCA1/2*-mutated breast cancers are highly sensitive to the clinical PARP inhibitor AZD2281 (olaparib). No results are available for sporadic breast cancers with epigenetic silencing of *BRCA1* via promoter hypermethylation, even though in vitro studies indicate sensitivity of *BRCA1*-methylated cell lines to PARP inhibitors (14,19).

Although most alkylating agents or PARP inhibitors show good initial responses, tumor relapses and resistance often occur (5,16,18,20). One resistance mechanism described in *BRCA* mutation carriers involves restoration of HR capacity through additional *BRCA* mutations that lead to restoration of the open reading frame and BRCA re-expression (21–24). Little information is available about resistance mechanisms in *BRCA1*-methylated tumors.

Because HRD-targeting therapies will likely become important in the treatment of BRCA1-deficient tumors, it is essential to gain knowledge of resistance mechanisms to these therapeutics. We therefore developed patient-derived xenograft (PDX) models of TNBC and used these models to study response and resistance to different alkylating agents and PARP inhibitors.

ARTICLE

Methods

Patient-Derived Xenograft (PDX) Models

Mouse experimental procedures were approved by the Netherlands Cancer Institute animal experiments committee and were performed according to institutional regulations. Fragments of human breast tumors obtained with approval of the Translational Research Board of the Netherlands Cancer Institute were engrafted into the fourth mammary fat pad of six-week-old female Swiss nude mice (25). After tumor outgrowth, tumor size was measured twice per week, and tumor volume calculated (0.5 x length x width^2). When tumors reached a size of 700 to 1000 mm^3, pieces were collected for serial transplantation. Additional pieces were snap-frozen or fixed in formalin. Details are provided in the Supplementary Methods (available online).

Intervention Studies

Mice were randomly assigned to treatment groups when tumor volume reached 100 mm^3. When tumors were approximately 200 mm^3, mice were left untreated or treated with cisplatin (6 mg/kg i.v., once every 2 weeks), melphalan (10 mg/kg i.p., once every 2 weeks), nimustine (15 mg/kg i.p., once every week), or olaparib (50 mg/kg i.p., daily) in a nonblinded fashion. Treatments were stopped if tumors regressed to less than 50% of start size and were resumed when tumors relapsed to start size. Mice were killed by CO_2 asphyxiation in case of drug toxicity or when tumors reached a maximum size of 1500 mm^3.

DNA and RNA Isolation

Genomic DNA was isolated from snap-frozen tumor tissue using proteinase-K lysis and organic extraction or from formalin-fixed, paraffin-embedded (FFPE) material using the QIAamp DNA FFPE tissue kit (Qiagen, Venlo, the Netherlands). Total RNA was isolated from snap-frozen tissue using RNA-Bee or from FFPE material using the High Pure FFPE RNA micro kit (Roche, Almere, the Netherlands). Patients were treated as part of ongoing clinical trials (NCT01057069 and older). Trials were approved by the ethics committee, and informed consent was obtained. Neoadjuvant chemotherapy consisted of six doses of AC (adriamycin/cyclophosphamide) or three doses of CD (capecitabine/docetaxel) followed by six doses of AC. Details are provided in the Supplementary Methods (available online).

Quantitative Reverse Transcription Polymerase Chain Reaction Analysis

cDNA was produced using Superscript II (Invitrogen, Landsmeer, the Netherlands) and random hexamers as primers. Taqman assays were used for analysis of *BRCA1* mRNA levels (Hs0173233_m1 and Hs01556193_m1). *GAPDH* (4326317E) or *ACTB* (4310881E) were used for normalization.

BRCA1 Promoter Methylation

BRCA1 promoter hypermethylation was measured using methylation-specific polymerase chain reaction (PCR) as described previously (3) or by MS-MLPA (MRC Holland, Amsterdam, the Netherlands) according to manufacturer's instructions.

Immunoblot Analysis

Fresh-frozen tumor was lysed in RIPA buffer for 10 minutes on ice. Samples were centrifuged (4 °C, 10 minutes), and the supernatant used to determine protein concentration. Eighty μg of total protein was heated for five minutes at 95 °C in NuPAGE LDS sample buffer, separated on NuPAGE Novex 3%-8% Tris-Acetate gels and blotted onto Immobilon-P membrane. Membranes were blocked with 5% nonfat dried milk and stained with anti-BRCA1 antibody (#9010, Cell Signaling, Leiden, the Netherlands). Blots were subsequently incubated with goat-anti-rabbit-HRP (DAKO, Heverlee, Belgium), washed, and incubated with ECL-plus chemiluminescence solution (Amersham, Eindhoven, the Netherlands). Details are provided in the Supplementary Methods (available online).

Kinome Sequencing

DNA libraries were prepared using the TruSeq DNA Sample Preparation Kit (Illumina, Eindhoven, the Netherlands). Genomic DNA (1.4μg) was fragmented to an average size of 200 bp, end-repaired, and A-tailed. Libraries were amplified with six to seven cycles of PCR. Pools of five libraries (100 ng of each library) were hybridized to RNA baits from the SureSelect Human Kinome Kit (Agilent) in the presence of custom blockers (blocker 1: 5′AGATCGGAAGAGCACACGTCTGAACTCCAGTCACNNNNNNATCTCGTATGCCGTCTTCTGCTT-G/3′ddC; blocker 2: 5′CAAGCAGAAGACGGCATACGAGATNNNNNNGTGACTGGAGTTCAGACGTGTGCTCTTCCGATCT/3′ddC). Enriched DNA was amplified with 11 cycles of PCR and sequenced on a HiSeq2000 (Illumina) using a 55 bp paired-end protocol (5-10 libraries/lane). Reads were aligned to the human (human_g1k_v37_decoy) and mouse (mm10) reference genomes using BWA mem (version 7.0.12). The human alignment was processed for duplicate marking, indel realignment, and base recalibration using Picard Tools (version 1.128) and GATK (version 3.4), as recommended by GATK best practices, and filtered to remove contaminating mouse reads using a tool called XenoFilteR (manuscript in preparation). Kinome sequencing data was used specifically to search for mutations in the *BRCA1* locus by visual inspection of reads using IGV. Mutations were validated using across-rearrangement PCR and Sanger sequencing.

PCR of *BRCA1* Rearrangements and Intragenic Deletions

Primers were designed (26) to amplify only sequences containing intragenic deletions in T250 olap1, cis3, cis5 (amplifying a 240 bp mutant fragment), and T250 cis1 (amplifying a 935 bp wildtype fragment and a 233 bp mutant fragment). To confirm DNA breakpoints in T127 tumors with *BRCA1* rearrangements, PCR was performed using primers spanning the breakpoints and PCR products were sequenced. Primer sequences are provided in the Supplementary Methods (available online).

5′ RACE PCR

5′ Rapid amplification of cDNA ends (RACE) PCR was performed using the GeneRacer kit (Invitrogen). RACE PCR products were cloned into the TOPO-TA vector, and at least 10 clones were sequenced for each sample. Primer sequences are provided in the Supplementary Methods (available online).

RAD51 Staining

Mice were killed 24 hours after drug treatment, and tumor pieces were fixed in formalin. Staining for RAD51 and geminin was done as described previously (27).

Statistics

Overall survival was calculated as time from first treatment to death from any cause. Breast cancer–specific survival was calculated as time from first treatment to death because of large tumor. Recurrence-free survival was calculated as time from first treatment to time of tumor relapse to treatment start size after initial shrinkage of tumor. Survival curves were compared using the log-rank test, with exact *P* values estimated by Monte Carlo simulation procedure. The simulation approach was based on 10 000 samples with starting seed value of 23456 and performed using Cytel Studio software version 10 (http://www.cytel.com/software-solutions). *P* values of less than .05 were considered statistically significant. All statistical tests were two-sided.

Results

Characterization of Tumor Models

We established PDX models of TNBC that closely resembled the primary carcinomas from which they were derived (Figure 1A; Supplementary Figure 1, available online). We tested BRCA1 expression in our PDX models and found that models T127 and T162 lacked BRCA1 mRNA and the protein expression (Figure 1, A and B) associated with *BRCA1* promoter hypermethylation (Figure 1, C and D). T250 tumors did express *BRCA1* mRNA but no BRCA1 protein (Figure 1, A and B). Sequence analysis of the *BRCA1* gene in T250 showed a 1 bp deletion at position c.2210 (Figure 1E), leading to a premature stop codon (Thr737LeufsX15). Exome sequencing also showed mutations in other genes, including *TP53* in most PDX models (Supplementary Table 1, available online). In contrast to multiple RAD51 foci seen in BRCA1-proficient T241 tumors, no RAD51 foci could be detected in the BRCA1-deficient models after induction of DSBs by cisplatin treatment, confirming loss of HR through BRCA1 dysfunction in these tumors (Figure 1F).

Sensitivity of BRCA1-Deficient PDX Tumors to Alkylators and Olaparib

We used our BRCA1-deficient PDX models to study BRCA1 deficiency in response to the alkylating agents cisplatin, melphalan, and nimustine and the PARP inhibitor olaparib. BRCA1-deficient tumors initially responded well to these agents, with volume reductions ranging from 75.0% to complete disappearance of palpable tumor (Supplementary Figure 2, available online). Most tumors relapsed but remained sensitive to additional treatment rounds. Out of 57 mice, 20 succumbed to drug-related toxicity after repeated treatment with alkylating agents (Supplementary Table 2, available online). We observed induction of resistance in 22 out of 57 BRCA1-deficient tumors treated with alkylating agents and in 15 out of 18 olaparib-treated tumors (Supplementary Figure 2 and Supplementary Table 2, available online).

Treatments led to substantially prolonged overall survival (log-rank test untreated vs treated $P < .001$ for T127, $P = .05$ for T162, $P = .002$ for T250) and breast cancer–specific survival (log-rank test untreated vs treated $P < .001$ for T127, $P < .001$ for T162, $P < .001$ for T250) in BRCA1-deficient PDX models (Figure 2, A-C). In contrast, BRCA1-proficient tumors showed no statistically significant treatment response (Figure 2D; Supplementary Figure 2, available online).

Intragenic *BRCA1* Deletions in Therapy-Resistant *BRCA1*-Mutated PDX Tumors

To determine whether acquired resistance in *BRCA1*-mutated T250 tumors is a stable trait, we transplanted and retreated pieces from resistant T250 tumors. Six out of seven tumor outgrowths remained resistant to treatment and showed cross-resistance to other agents (Figure 3A). Immunoblot analysis of BRCA1 expression in 14 therapy-resistant T250 tumors showed

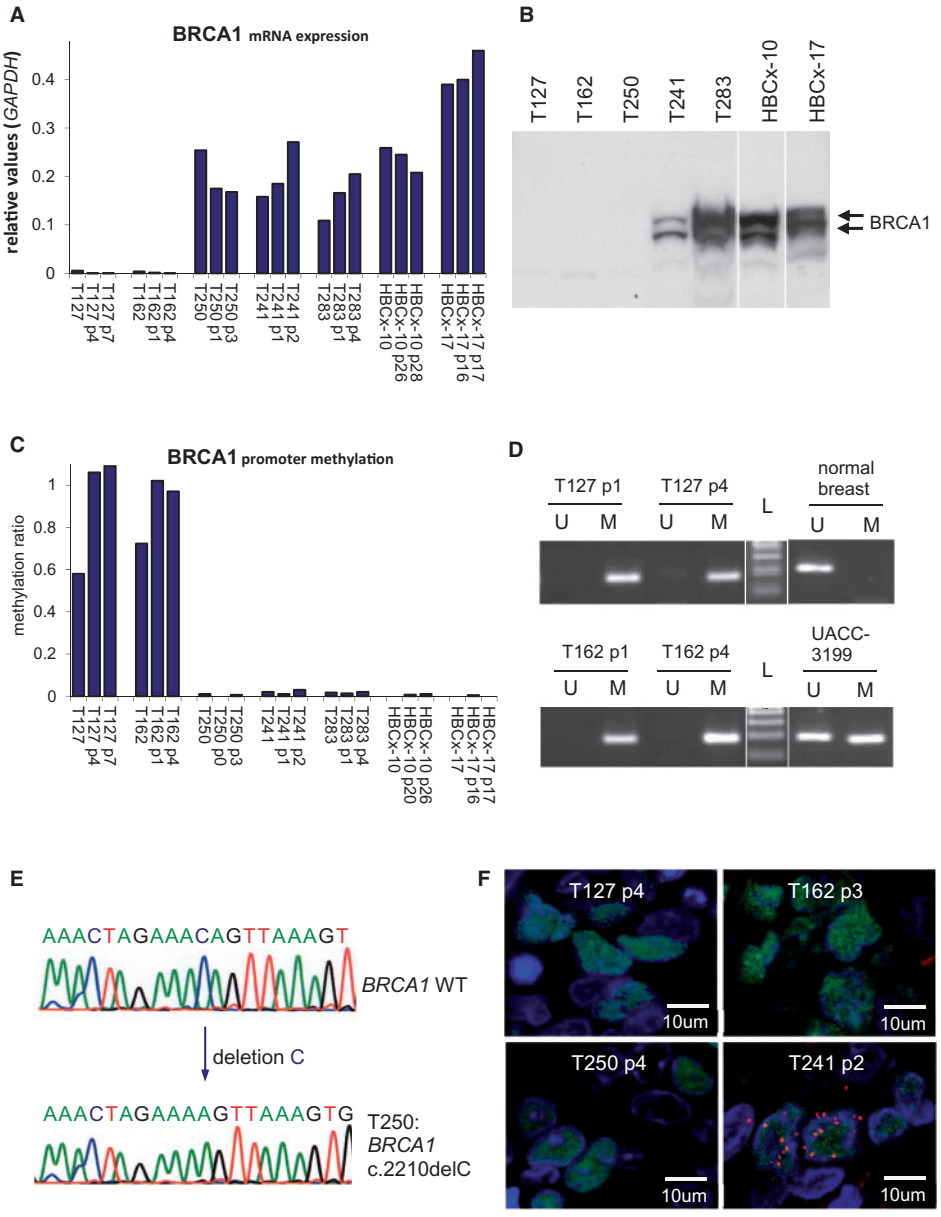

Figure 1. BRCA1 expression and RAD51 focus formation in patient-derived xenograft (PDX) models of triple-negative breast cancer (TNBC). **A)** *BRCA1* mRNA expression in seven PDX models of TNBC (T127, T162, T250, T241, T283, HBCx-10, and HBCx-17). *BRCA1* mRNA expression was measured in primary human tumor tissue (no passage number shown) and the corresponding PDX tumors of different passages (p1-p28). **B)** Immunoblot analysis of BRCA1 protein expression in seven PDX models (T127, T162, T250, T241, T283, HBCx-10, and HBCx-17), showing absence of full-length BRCA1 protein in T127, T162, and T250. **C)** Analysis of *BRCA1* promoter hypermethylation in seven PDX models measured using methylation-specific multiplex ligation-dependent probe amplification (MS-MLPA). Methylation was measured in primary human tumor tissue (no passage number shown) and the corresponding PDX tumors of different passages (p1-p26). **D)** Analysis of *BRCA1* promoter hypermethylation in PDX models T127 and T162 by methylation-specific PCR (MSP). p1-p4 indicate passage number of the PDX tumors. PCR product in the lane marked "U" indicates unmethylated *BRCA1* promoter region; product in lane marked "M" indicates presence of methylated sequences. UACC-3199 was used as positive control for the methylated *BRCA1* promoter, and normal breast tissue was used as a control for the unmethylated *BRCA1* promoter. L: 100 bp DNA ladder. **E)** DNA sequence analysis of *BRCA1* in normal breast (wild-type sequence) and T250 primary tumor, showing deletion of C at position c.2210 in this tumor. **F)** Low levels of DNA damage–induced RAD51 focus formations in BRCA1-deficient PDX tumors T127, T162, and T250, sampled 24 hours after a single cisplatin treatment. Tumor passage number is indicated by p2-p4. RAD51 staining is shown in **red**, and geminin staining in **green**. DAPI **(blue)** is used as a counterstain. A high level of RAD51 focus formation is seen in the BRCA1-proficient PDX tumor T241. See also Supplementary Figure 1 and Supplementary Table 1 (available online).

that eight of these tumors re-expressed BRCA1 (Figure 3B) and formed high levels of RAD51 foci after DSB induction (Figure 3C). Sequencing of the *BRCA1* gene showed additional deletions in the region surrounding the c.2210delC founder mutation (Figure 3D). Seven out of eight tumors showed small (6-24 bp) deletions whereas one cisplatin-resistant tumor contained a 702 bp deletion. All additional deletions encompassed the c.2210delC mutation and restored the *BRCA1* open reading frame (Figure 3E; Supplementary Figure 3, available online). PCR using primers that only amplify sequences with additional mutations (21)

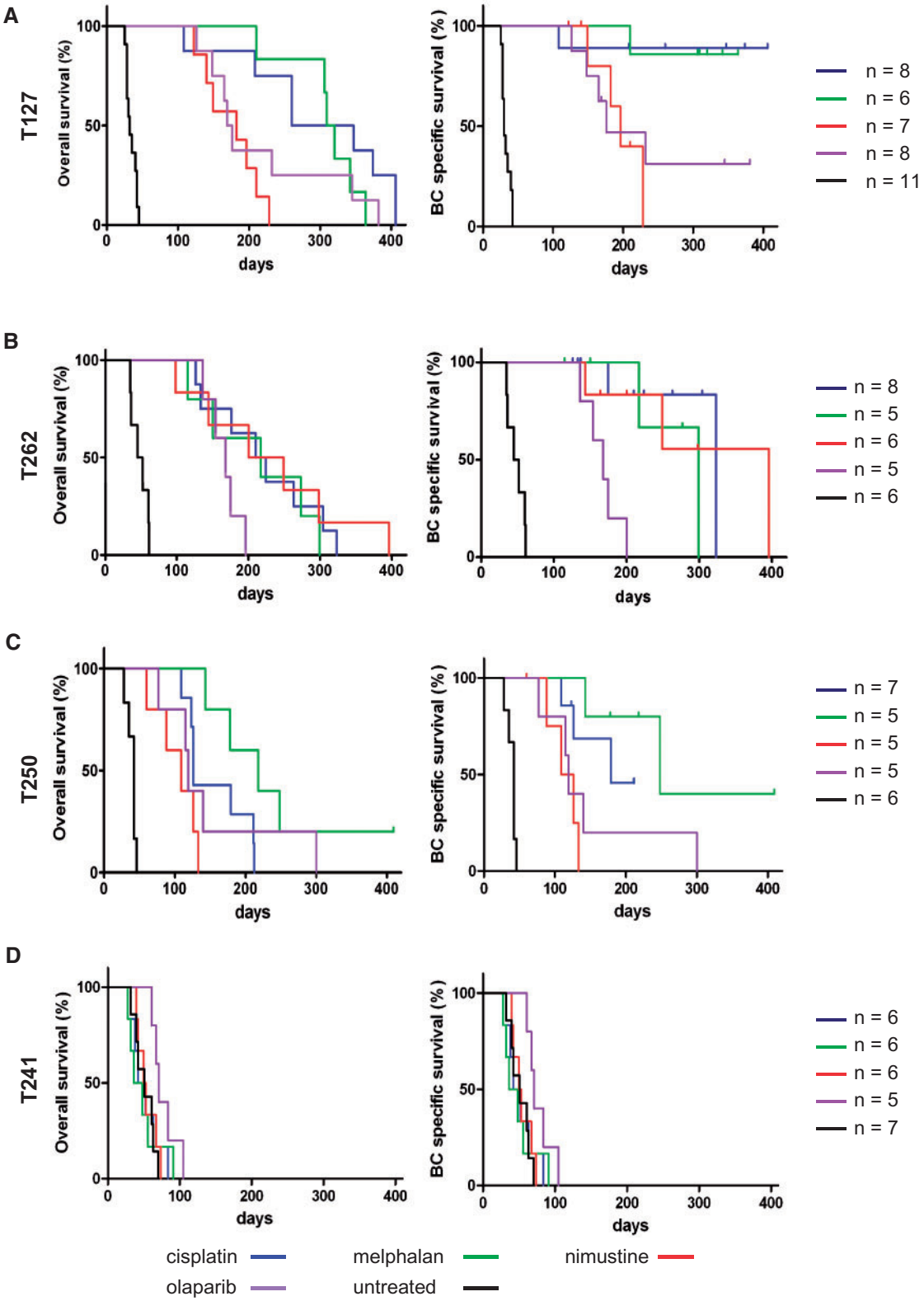

Figure 2. Effects of treatment with alkylators or olaparib on survival of mice with BRCA1-deficient patient-derived xenograft (PDX) tumors. Graphs showing overall survival (OS; left) and breast cancer–specific survival (BCSS; right) of mice bearing BRCA1-deficient or -proficient PDX tumors treated with cisplatin (blue), melphalan (green), nimustine (red), or olaparib (purple) or left untreated (black). Numbers of mice treated are shown for each curve. **A)** T127 (OS: log-rank test untreated vs treated $P < .001$; BCSS: log-rank test untreated vs treated $P < .001$). **B)** T162 (OS: log-rank-test untreated vs treated $P = .05$; BCSS: log-rank test untreated vs treated $P < .001$). **C)** T250 (OS: log-rank test untreated vs treated $P = .002$; BCSS: log-rank test untreated vs treated $P < .001$). **D)** T241 (OS: log-rank test untreated vs treated $P = .08$; BCSS: log-rank test untreated vs treated $P = .08$). All statistical tests were two-sided. See also Supplementary Figure 2 and Supplementary Table 2 (available online).

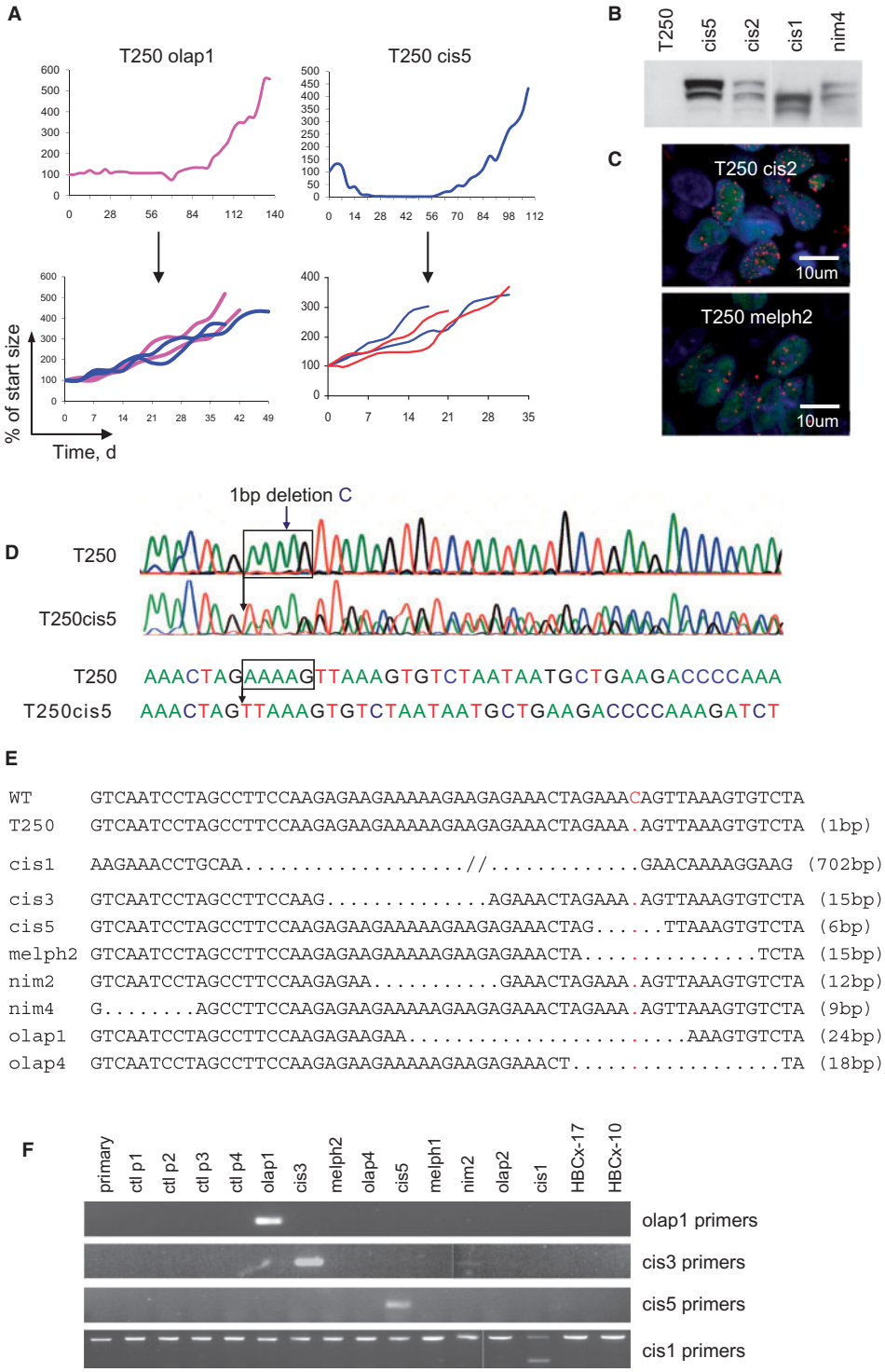

Figure 3. Intragenic *BRCA1* deletions in therapy-resistant *BRCA1*-mutated patient-derived xenograft (PDX) tumors. **A)** Response of T250olap1 and T250cis5 tumors to olaparib (pink) or cisplatin (blue) treatment (top). At time of death, tumor pieces were transplanted and treated again after outgrowth (bottom). Tumors were treated with olaparib (pink; once every day), cisplatin (blue; once every 2 weeks), or nimustine (red; once every week) as long as tumor size was larger than 50% of the tumor at start of treatment or when relapsed tumors grew back to the starting size. **B)** Immunoblot analysis of BRCA1 expression in untreated and therapy-resistant T250 tumors. **C)** Cisplatin-induced RAD51 focus formation in therapy-resistant T250 tumors. RAD51 staining is shown in red, and geminin staining in green. DAPI (blue) is used as a counterstain. **D)** Example of secondary *BRCA1* mutations in a treatment-resistant T250 tumor. Sequence chromatograms are shown for untreated T250 (containing a c.2210delC mutation) and T250 cis5. The box indicates the reading frame-restoring 5 bp deletion in T250cis5. **E)** Sequence analysis of *BRCA1* in normal tissue (WT), untreated T250 tumor, and eight therapy-resistant T250 tumors, showing additional intragenic *BRCA1* deletions in resistant tumors. Deleted bases are depicted by dots. Total numbers of deleted basepairs are shown behind each sequence. For T250cis1, an additional 670 bp of deleted *BRCA1* sequence is depicted by //. **F)** Polymerase chain reaction using deletion-specific primers for T250olap1, T250cis3, T250cis5, and primers spanning the 702 bp deletion in T250cis1, showing presence of additional *BRCA1* deletions in resistant T250 PDX tumors but not in the primary human tumor, untreated T250 tumors of several passages (ctrl p1-p4), or other therapy-resistant T250 tumors. HBCx-17 and HBCx-10 were used as negative controls for the presence of deletion-specific product. See also Supplementary Figure 3 (available online).

ARTICLE

detected secondary mutations in the resistant tumors but not the primary or any untreated PDX tumors tested (Figure 3F). These results indicate that development of resistance is associated with de novo deletions in *BRCA1*, leading to re-expression of BRCA1 in a subset of *BRCA1*-mutated PDX tumors.

BRCA1 Expression in Therapy-Resistant Tumors and Tumor Remnants of BRCA1-Methylated PDX Models

Also, therapy-resistant *BRCA1*-methylated tumors showed stable (cross-) resistance after transplantation (Figure 4A, left). Surprisingly, transplantation of tumor remnants from mice that had to be killed because of drug-related toxicity led in five out of 14 cases to outgrowths that did not shrink after treatment, indicating that resistance already developed in these tumor remnants (Figure 4A, middle, right). Thus, in total, we obtained 42 resistant tumors (14 tumors from the BRCA1-mutated PDX model T250, and 28 tumors from the BRCA1-methylated PDX models T127 and T162). We observed re-expression of *BRCA1* mRNA and protein in 18 out of 23 therapy-resistant tumors and five out of 5 resistant outgrowths from transplantable remnants (Figure 4, B and C). Of the 23 BRCA1-expressing therapy-resistant tumors, 16 showed demethylation of the *BRCA1* promoter while no *BRCA1* promoter demethylation was found in untreated tumors ($n = 8$) or therapy-resistant tumors ($n = 5$) that did not express BRCA1 (Figure 4B; Supplementary Figure 4, available online). In contrast to therapy-sensitive tumors, BRCA1-expressing resistant tumors showed RAD51 foci after DSB induction (Figure 4D), indicating that development of resistance in these tumors is associated with restoration of HR through *BRCA1* promoter demethylation and re-expression of BRCA1.

We did not observe other resistance mechanisms that were previously identified in BRCA-deficient cell lines and tumors from genetically engineered mouse models (Supplementary Figure 4, available online) (5,6,28–30). We also did not find any mutations in *BRCA1* in therapy-resistant tumors of *BRCA1*-methylated PDX models (data not shown).

BRCA1 Promoter Methylation and mRNA Expression in Patient Tumors

Next, we tested whether the resistance mechanisms we uncovered in our PDX models also occured in TNBC patients. In a series of 103 pretreatment biopsy samples from TNBC patients who received neoadjuvant chemotherapy, we detected *BRCA1* promoter methylation in 26 patients (25.2%), of whom 17 showed pathologic complete response after neoadjuvant chemotherapy and nine showed partial or no response, with vital tissue left at time of surgery (Supplementary Figure 5, available online). For three patients who showed a partial response, we obtained DNA from postsurgery tumor tissue, and from two of these patients we also obtained RNA. *BRCA1* promoter methylation and very low levels of *BRCA1* mRNA expression were found in pretreatment tumor tissue in these patients (Figure 5). Compared with pretreatment tissue, posttreatment tissue showed a two- to 66-fold decrease in *BRCA1* promoter methylation (Figure 5A) and a 12- to 28-fold increase in *BRCA1* mRNA levels (Figure 5B), indicating that BRCA1 re-expression via loss of promoter methylation might also underlie clinical resistance of *BRCA1*-methylated TNBCs to chemotherapy drugs.

BRCA1 Gene Fusions in Therapy-Resistant BRCA1-Methylated PDX Tumors

Although loss of *BRCA1* promoter methylation was observed in 16 out of 23 therapy-resistant T127 and T162 PDX tumors with BRCA1 re-expression, seven resistant tumors still showed *BRCA1* promoter hypermethylation. Using 5′ RACE PCR, we found *BRCA1* fusion transcripts in two tumors with high levels of BRCA1 (T127cis1 and T127nim2). We performed target locus amplification (TLA) (31) to identify additional genomic rearrangements at the *BRCA1* locus. Using TLA, we confirmed a rearrangement in T127cis1 and found rearrangements in two additional resistant tumors (T127nim1 and T127olap2) (Supplementary Figure 6A, available online). In all four tumors, fusion partners for *BRCA1* were located on chromosome 17 (Figure 6A). In three tumors, the exact genomic location of the breakpoints could be determined (Figure 6B). Mate pair sequencing showed a duplication of *BRCA1* in T127cis1 (Supplementary Figure 6, B and C, available online).

To determine if *BRCA1* rearrangements were already present in a subpopulation of cells in untreated tumors, we performed PCR analysis with rearrangement-specific primers. We detected the presence of rearrangements in the resistant tumors but not in the primary tumor or untreated T127 (Figure 6C) and T250 PDX tumors (Figure 3F).

We sequenced reverse transcription PCR (RT-PCR) products of *BRCA1* fusion transcripts to identify the exact fusion points. We found that the first base of *BRCA1* exon 2 was fused to the last base of exon 1 of *STAT3* and *CRLF3* in T127cis1 and T127nim1, respectively, and to the last base of exon 3 of *ACACA* in T127nim2 (Figure 6D, left). Immunoblot analysis showed the presence of full-length BRCA1 protein in resistant T127 tumors (Figure 4C).

RT-PCR specific to the *BRCA1* fusions detected rearrangements in the therapy-resistant T127 tumors, in which the rearrangements were originally detected but not in untreated tumors or other resistant tumors (Figure 6D, right). These results point to the development of de novo *BRCA1* rearrangements, leading to re-expression of BRCA1 as a mechanism of resistance in these tumors.

Characteristics of BRCA1 Breakpoints in Therapy-Resistant PDX Tumors

To characterize the rearrangement mechanism in the resistant tumors, we analyzed sequences of all breakpoints (Figure 7). We found 1 to 7 bp microhomologies in five of eight breakpoints in T250 tumors, and three of three breakpoints in T127 tumors (Figure 7). Insertion of nontemplated nucleotides was not found. Although some repetitive elements were found to overlap with the breakpoints, no larger stretches of homology were found in any of the tumors.

Discussion

We describe the use of PDX models of BRCA1-deficient TNBC to uncover novel mechanisms of therapy resistance. Although similar studies have been performed in genetically engineered mouse models (GEMMs) (6), these models contain large *Brca1* deletions that do not mimic the *BRCA1* germline mutations in patients (8,9). Furthermore, GEMMs cannot be used to model epigenetic inactivation of BRCA1, which occurs in approximately 15% of TNBCs and 11% to 15% of serous ovarian

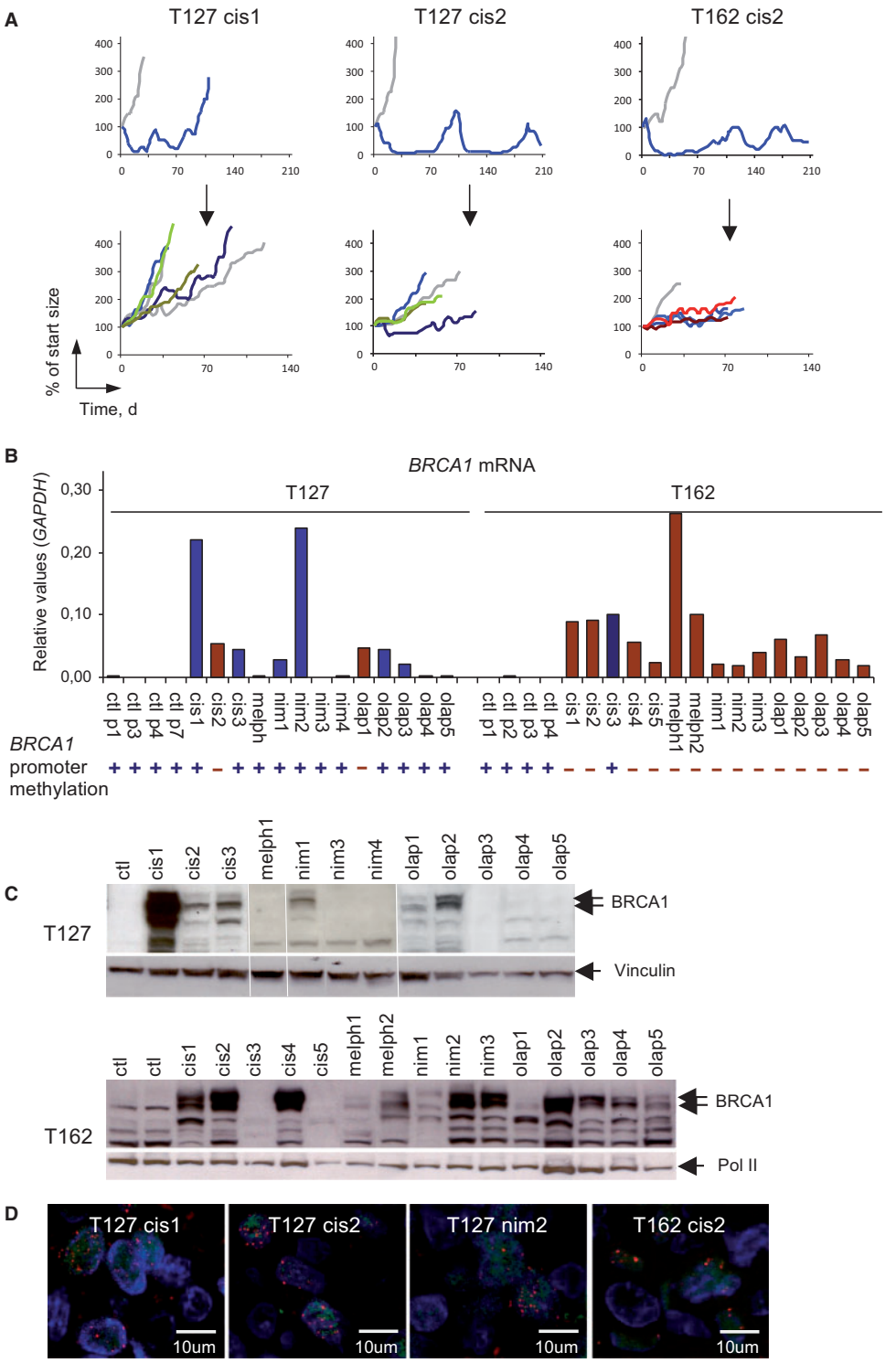

Figure 4. Therapy resistance in patient-derived xenograft (PDX) tumors with *BRCA1* promoter hypermethylation. **A)** Response to cisplatin in three *BRCA1*-methylated PDX tumors treated with cisplatin (top). At time of death, tumor pieces were transplanted and the resulting tumor outgrowths were again treated with cisplatin (blue), melphalan (green), or nimustine (red) or were left untreated (gray) (bottom). B) *BRCA1* mRNA expression in untreated and therapy-resistant T127 and T162 tumors after treatment with cisplatin (cis), melphalan (melph), nimustine (nim), or olaparib (olap). Ctrl indicates untreated control tumors; p1-p7 indicates passage number of control tumors. *BRCA1* mRNA levels are normalized to *GAPDH* mRNA levels. Red bars indicate tumors with loss of *BRCA1* promoter hypermethylation, which are marked with "–". **Blue bars** indicate tumors with retention of *BRCA1* promoter hypermethylation, which are marked with "+". **C)** Immunoblot showing expression of BRCA1 protein in therapy-resistant T127 and T162 PDX tumors. Ctrl indicates untreated control PDX tumor. Vinculin and Pol II were used as loading controls. **D)** Cisplatin-induced RAD51 focus formation in therapy-resistant PDX tumors T127cis1, T127cis2, T127nim2, and T162cis2. See also Supplementary Figure 4 (available online).

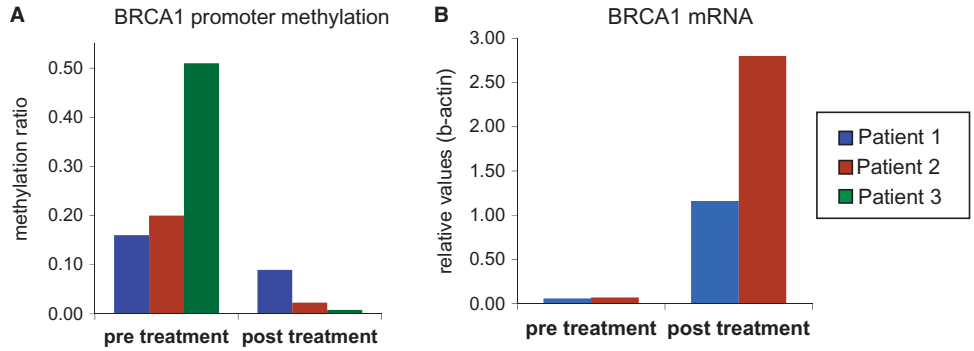

Figure 5. *BRCA1* promoter methylation and mRNA expression in patient samples before and after neoadjuvant chemotherapy. **A)** *BRCA1* promoter methylation as measured by MS-MLPA and *BRCA1* mRNA levels **(B)** in pretreatment biopsies and post-treatment surgery material of patients with triple-negative breast cancer. No RNA was available to measure *BRCA1* mRNA levels in patient 3. *BRCA1* mRNA levels were normalized to *ACTB*. See also Supplementary Figure 5 (available online).

carcinomas (32,33). Preclinical studies have been performed in *BRCA1*-methylated breast cancer cell line xenografts (19), but these cell lines have lost many features of the original breast tumors (34).

Unlike cancer cell lines, PDX models preserve the characteristics of the patient tumors from which they are derived (25,35,36). Additionally, these models provide the opportunity to test the effects of different treatments on the same tumor. We show that clinically relevant breast cancer subgroups such as BRCA1-deficient TNBCs can be identified in panels of PDX models and used to advance our understanding of therapy response and resistance.

HRD-targeting therapeutics such as platinum drugs and PARP inhibitors have shown favorable responses in patients with *BRCA1*-associated hereditary cancer (8,9,17,18), but they may also be useful for treating patients with BRCA1-deficient sporadic cancer. Studies in sporadic TNBC patients have shown that *BRCA1* promoter methylation correlates with good response to neoadjuvant cisplatin treatment (10) although varying results have been reported for adjuvant chemotherapy (37,38). Preclinical studies show increased sensitivity of *BRCA1*-methylated tumor cell lines to olaparib and other PARP inhibitors (14,19,39), but no information is available from clinical studies. We find that BRCA1-deficient PDX tumors show excellent initial responses to alkylating agents and the clinical PARP inhibitor olaparib. Responses of the *BRCA1*-methylated PDX tumors are comparable with those of the *BRCA1*-mutated model, indicating that *BRCA1* promoter methylation is a good biomarker for sensitivity to alkylating agents or PARP inhibitors in the tested models.

Despite their initial sensitivity to HRD-targeting therapeutics, most BRCA1-deficient PDX tumors relapse and eventually acquire resistance. In most PDX tumors, resistance is associated with re-expression of BRCA1. In the BRCA1-c.2210delC model, more than half of the therapy-resistant tumors restored the *BRCA1* open reading frame via acquisition of additional *BRCA1* deletions spanning the germline mutation. These types of secondary mutations have previously been described in therapy-resistant *BRCA1/2*-mutated breast and ovarian tumors (21–24,33), underscoring the utility of PDX models for identification of clinically relevant resistance mechanisms. The presence of a large (702 bp) reading frame-restoring deletion in one cisplatin-resistant BRCA1-c.2210delC tumor demonstrates that this part of the BRCA1 protein (comprising AA 670-904) is not required for driving therapy resistance.

In line with cell line studies (14,40), a number of *BRCA1*-methylated PDX tumors acquired therapy resistance via re-expression of BRCA1 because of the loss of the *BRCA1* promoter methylation. Similar to what was shown in a patient with ovarian carcinoma (33), we demonstrated *BRCA1* promoter demethylation and mRNA re-expression in samples from TNBC patients after neoadjuvant chemotherapy, indicating that this mechanism may be relevant to the development of clinical resistance in patients with *BRCA1*-methylated TNBC. In other *BRCA1*-methylated PDX tumors, BRCA1 re-expression was driven by de novo intrachromosomal genomic rearrangements by which *BRCA1* transcription is placed under the control of a heterologous promoter, similar to the *MDR1* gene fusions observed in in vitro studies (41) and in ovarian cancer patients (33). This novel finding demonstrates that BRCA1 re-expression in therapy-resistant *BRCA1*-methylated tumors may be driven by epigenetic as well as genetic mechanisms.

Chromosomal rearrangements of BRCA1-deficient tumor cells are thought to be caused by error-prone DSB repair pathways such as nonhomologous end-joining (NHEJ) or microhomology-mediated end-joining (MMEJ) (43). In line with this, analysis of the *BRCA1* gene rearrangements in therapy-resistant PDX tumors revealed no large regions of homology but mostly small deletions or microhomology in the breakpoints. This excludes nonallelic HR as a mechanism of breakpoint formation (42) but is consistent with NHEJ or MMEJ (43). One tumor showed a more complex rearrangement consisting of a tandem duplication. It is unclear whether this duplication is caused by NHEJ or by alternative mechanisms such as fork stalling and template switching (42).

Therapy resistance may be induced by de novo (epi)genetic alterations or result from selective outgrowth of pre-existing resistant tumor cells (21,44). We did not detect pre-existing resistant cells in any of the primary or untreated tumors, even when using highly sensitive nested PCRs. Although we cannot exclude the possibility that detection of pre-existing resistant cells is obscured by very low abundance or by intratumor heterogeneity, our results suggest that acquired resistance in our models is driven by de novo rather than pre-existing mutations. In line with this, mice had to be treated for multiple rounds before resistant tumors emerged, and none of the resistance-associated mutations were found in multiple resistant tumors derived from the same donor.

Collectively, our results provide insight into resistance mechanisms in BRCA1-deficient breast tumors. A limitation of our study was the relatively small number of PDX models we used because of the time-consuming and labor-intensive nature of producing PDX models and the long-term intervention studies required to induce resistance. Additionally, we have been

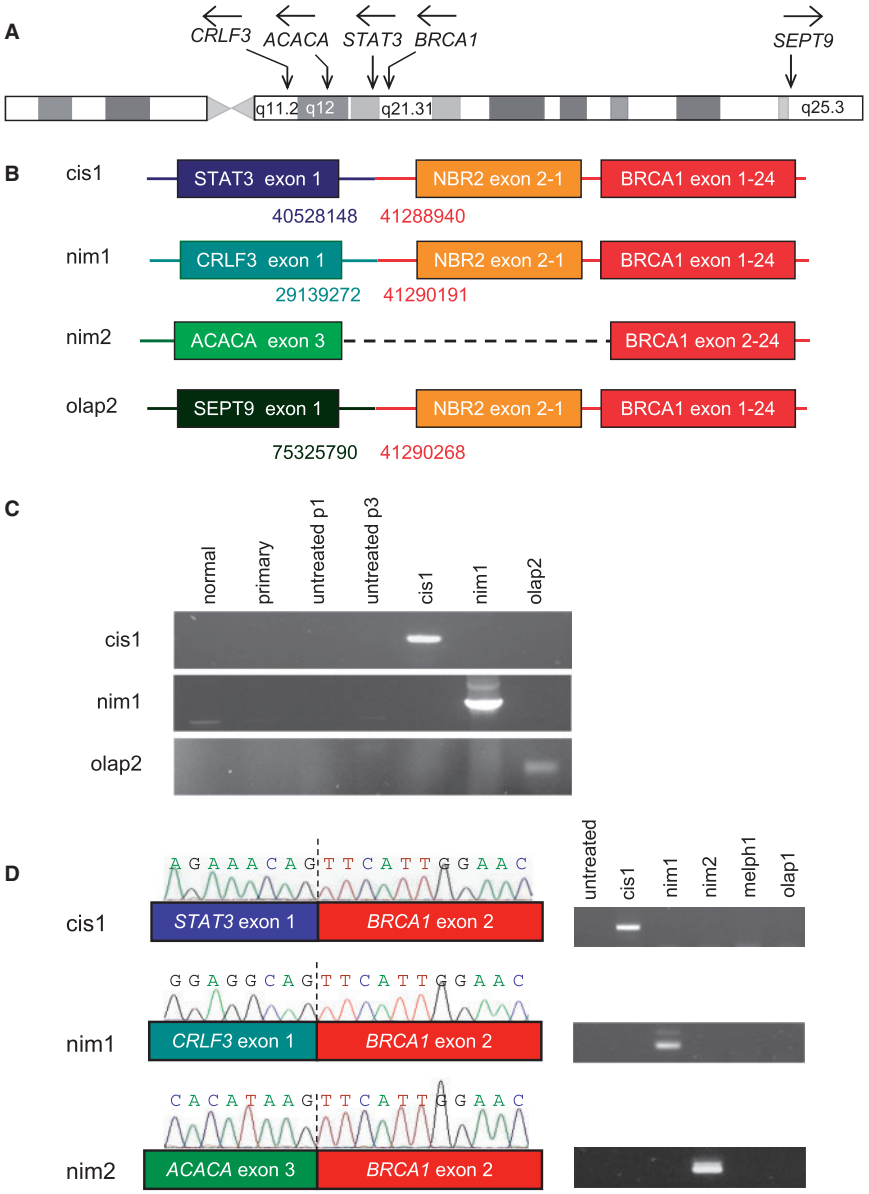

Figure 6. *BRCA1* gene fusions in therapy-resistant patient-derived xenograft (PDX) tumors with *BRCA1* promoter hypermethylation. **A)** Schematic representation of chromosome 17 showing the genomic locations and transcriptional orientation of *ACACA*, *STAT3*, *CRLF3*, *SEPT9*, and *BRCA1*. **B)** Schematic representation of genomic fusions in T127 cis1, nim1, nim2, and olap2 tumors. Numbers indicate the chromosomal coordinates for the genomic sequences that form either side of the fusion point. For T127 nim2, the region between *BRCA1* exon 2 and *ACACA* exon 3 is indicated by a dashed line because the exact chromosomal coordinates could not be determined. **C)** Polymerase chain reaction (PCR) using primers spanning the T127 cis1, nim1, and olap2 breakpoints performed on normal patient DNA, primary tumor DNA, and DNA from two untreated T127 PDX tumors (p0, p2) and from T127cis1, nim1, and olap2. **D)** Analysis of expression of chimeric *BRCA1* transcripts in therapy-resistant T127 PDX tumors with retention of *BRCA1* promoter methylation (left). Left panels show schematic representation of first exons of fusion transcripts in T127 cis1, nim1, and nim2. RNA sequences containing the point of fusion are also shown. Right panels show results for reverse transcription PCR using primers that span the breakpoints in a series of untreated and resistant T127 tumors. We were unable to detect a product in T127olap2 possibly because of the low level of *BRCA1* expression. *BRCA1*: ENST00000357654, *STAT3*: ENST00000264657, *CRLF3*: ENST00000324238, *ACACA*: ENST00000353139. See also Supplementary Figure 5 (available online).

unable to determine mechanisms underlying resistance in tumors that do not show BRCA1 re-activation. Further work will be required to identify these mechanisms.

Funding

This research was supported by grants from the Dutch Cancer Society (NKI 2011-5197 and EMCR 2014-7048); the Netherlands Organization for Scientific Research (NWO-NGI Zenith 93512009 and NWO-ZonMW Vici 91814643); the EurocanPlatform network of excellence, funded by the EU Seventh Framework Programme; the CombatCancer synergy project, funded by the European Research Council; and the Cancer Genomics Netherlands gravitation programme and Cancer Systems Biology Center (CSBC), funded by the NWO.

Notes

The study funders had no role in the design of the study; the collection, analysis, or interpretation of the data; the writing of

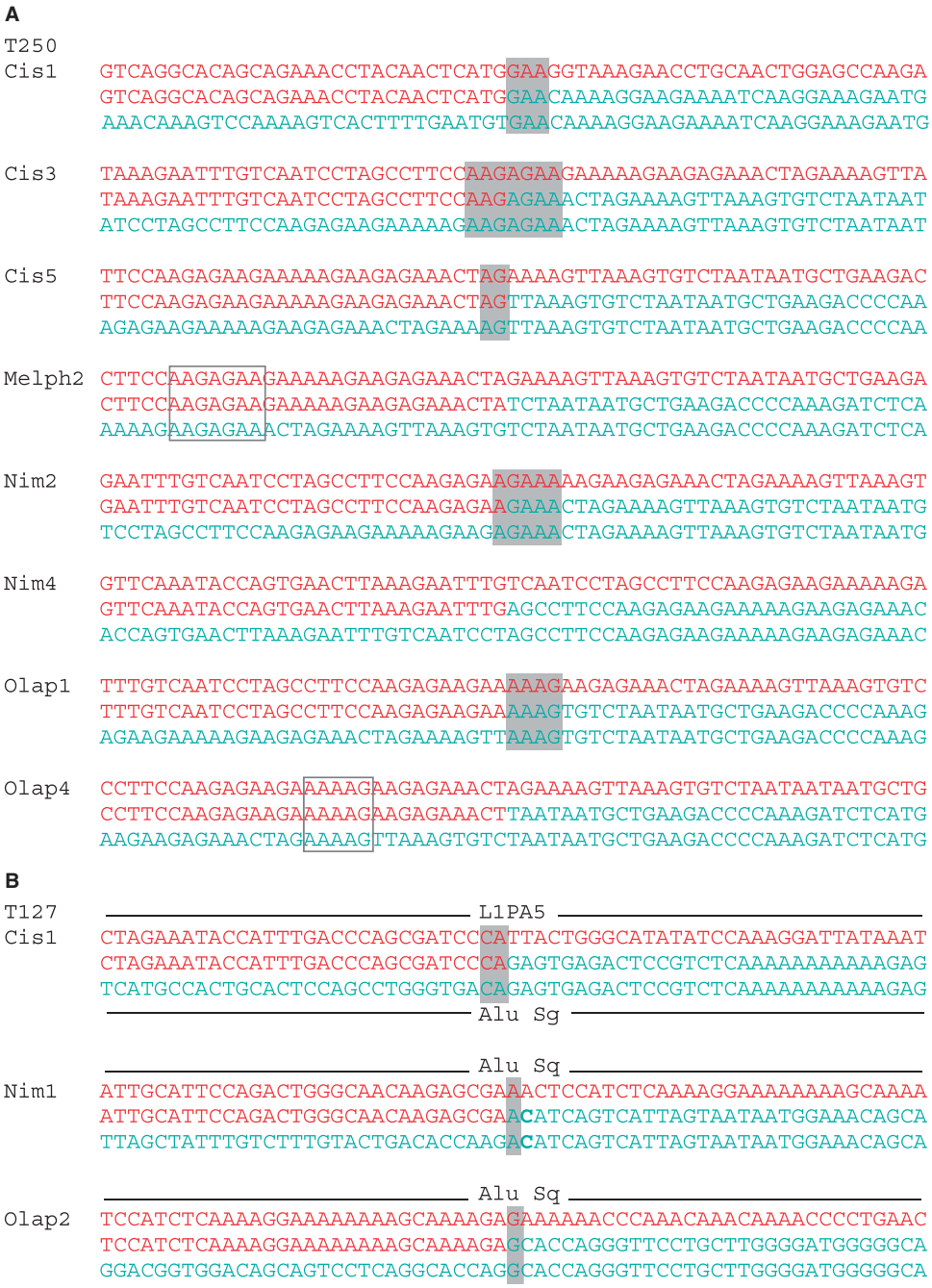

Figure 7. Characterization of *BRCA1* breakpoints in resistant T250 and T127 tumors. Sequence alignments are shown for intragenic *BRCA1* deletions in resistant T250 tumors **(A)** and rearrangements in the *BRCA1* locus in resistant T127 tumors **(B)**. Nucleotides highlighted in gray represent presence of microhomology at the breakpoint; gray boxes highlight areas of microhomology (>5 bp) close to the breakpoint. If present, repetitive elements are shown above and below sequences. For T250, proximal sequence is shown in red, and distal sequence in green. For T127, sequence of *NBR2* intron is shown in red whereas *STAT3* (cis1), *CRLF3* (nim1), and *SEPT9* (olap2) sequences are shown in green.

the manuscript; or the decision to submit the manuscript for publication. The authors have declared that no conflict of interest exists.

We thank the personnel of the Netherlands Cancer Institute animal facilities for excellent animal care; the departments of Pathology and Animal Pathology at the NKI and Marick Laé at the Curie Institute for assistance in immunohistochemical stainings; Roelof Pruntel for assistance in DNA sequence analysis of revertant tumors; Mark O'Connor (AstraZeneca) for providing olaparib; and Piet Borst and Sven Rottenberg for critically reading the manuscript.

References

1. Foulkes WD, Smith IE, Reis-Filho JS. Triple-negative breast cancer. *N Engl J Med*. 2010;363(20):1938–1948.
2. Rice JC, Ozcelik H, Maxeiner P, et al. Methylation of the BRCA1 promoter is associated with decreased BRCA1 mRNA levels in clinical breast cancer specimens. *Carcinogenesis*. 2000;21(9):1761–1765.

ARTICLE

3. Esteller M, Silva JM, Dominguez G, et al. Promoter hypermethylation and BRCA1 inactivation in sporadic breast and ovarian tumors. *J Natl Cancer Inst*. 2000;92(7):564–569.
4. Alli E, Sharma VB, Hartman AR, et al. Enhanced sensitivity to cisplatin and gemcitabine in Brca1-deficient murine mammary epithelial cells. *BMC Pharmacol*. 2011;11:7.
5. Rottenberg S, Jaspers JE, Kersbergen A, et al. High sensitivity of BRCA1-deficient mammary tumors to the PARP inhibitor AZD2281 alone and in combination with platinum drugs. *Proc Natl Acad Sci U S A*. 2008;105(44):17079–17084.
6. Rottenberg S, Nygren AO, Pajic M, et al. Selective induction of chemotherapy resistance of mammary tumors in a conditional mouse model for hereditary breast cancer. *Proc Natl Acad Sci U S A*. 2007;104(29):12117–12122.
7. Tassone P, Tagliaferri P, Perricelli A, et al. BRCA1 expression modulates chemosensitivity of BRCA1-defective HCC1937 human breast cancer cells. *Br J Cancer*. 2003;88(8):1285–1291.
8. Byrski T, Gronwald J, Huzarski T, et al. Pathologic complete response rates in young women with BRCA1-positive breast cancers after neoadjuvant chemotherapy. *J Clin Oncol*. 2010;28(3):375–379.
9. Byrski T, Huzarski T, Dent R, et al. Response to neoadjuvant therapy with cisplatin in BRCA1-positive breast cancer patients. *Breast Cancer Res Treat*. 2009;115(2):359–363.
10. Silver DP, Richardson AL, Eklund AC, et al. Efficacy of Neoadjuvant Cisplatin in Triple-Negative Breast Cancer. *J Clin Oncol*. 2010;28(7):1145–1153.
11. Lord CJ, Garrett MD, Ashworth A. Targeting the double-strand DNA break repair pathway as a therapeutic strategy. *Clin Cancer Res*. 2006;12(15):4463–4468.
12. Bryant HE, Schultz N, Thomas HD, et al. Specific killing of BRCA2-deficient tumours with inhibitors of poly(ADP-ribose) polymerase. *Nature*. 2005;434(7035):913–917.
13. Farmer H, McCabe N, Lord CJ, et al. Targeting the DNA repair defect in BRCA mutant cells as a therapeutic strategy. *Nature*. 2005;434(7035):917–921.
14. Veeck J, Ropero S, Setien F, et al. BRCA1 CpG island hypermethylation predicts sensitivity to poly(adenosine diphosphate)-ribose polymerase inhibitors. *J Clin Oncol*. 2010;28(29):e563–e564.
15. Evers B, Drost R, Schut E, et al. Selective inhibition of BRCA2-deficient mammary tumor cell growth by AZD2281 and cisplatin. *Clin Cancer Res*. 2008;14(12):3916–3925.
16. Hay T, Matthews JR, Pietzka L, et al. Poly(ADP-ribose) polymerase-1 inhibitor treatment regresses autochthonous Brca2/p53-mutant mammary tumors in vivo and delays tumor relapse in combination with carboplatin. *Cancer Res*. 2009;69(9):3850–3855.
17. Fong PC, Boss DS, Yap TA, et al. Inhibition of poly(ADP-ribose) polymerase in tumors from BRCA mutation carriers. *N Engl J Med*. 2009;361(2):123–134.
18. Tutt A, Robson M, Garber JE, et al. Oral poly(ADP-ribose) polymerase inhibitor olaparib in patients with BRCA1 or BRCA2 mutations and advanced breast cancer: a proof-of-concept trial. *Lancet*. 2010;376(9737):235–244.
19. Drew Y, Mulligan EA, Vong WT, et al. Therapeutic potential of poly(ADP-ribose) polymerase inhibitor AG014699 in human cancers with mutated or methylated BRCA1 or BRCA2. *J Natl Cancer Inst*. 2011;103(4):334–346.
20. Shafee N, Smith CR, Wei S, et al. Cancer stem cells contribute to cisplatin resistance in Brca1/p53-mediated mouse mammary tumors. *Cancer Res*. 2008;68(9):3243–3250.
21. Norquist B, Wurz KA, Pennil CC, et al. Secondary somatic mutations restoring BRCA1/2 predict chemotherapy resistance in hereditary ovarian carcinomas. *J Clin Oncol*. 2011;29(22):3008–3015.
22. Sakai W, Swisher EM, Karlan BY, et al. Secondary mutations as a mechanism of cisplatin resistance in BRCA2-mutated cancers. *Nature*. 2008;451(7182):1116–1120.
23. Swisher EM, Sakai W, Karlan BY, et al. Secondary BRCA1 mutations in BRCA1-mutated ovarian carcinomas with platinum resistance. *Cancer Res*. 2008;68(8):2581–2586.
24. Edwards SL, Brough R, Lord CJ, et al. Resistance to therapy caused by intragenic deletion in BRCA2. *Nature*. 2008;451(7182):1111–1115.
25. Marangoni E, Vincent-Salomon A, Auger N, et al. A new model of patient tumor-derived breast cancer xenografts for preclinical assays. *Clin Cancer Res*. 2007;13(13):3989–3998.
26. Wang Y, Rollin JA, Zhang YH. Enhancing allele-specific PCR for specifically detecting short deletion and insertion DNA mutations. *Mol Cell Probes*. 2010;24(1):15–19.
27. Graeser M, McCarthy A, Lord CJ, et al. A marker of homologous recombination predicts pathologic complete response to neoadjuvant chemotherapy in primary breast cancer. *Clin Cancer Res*. 2010;16(24):6159–6168.
28. Gupta A, Lutsenko S. Human copper transporters: mechanism, role in human diseases and therapeutic potential. *Future Med Chem*. 2009;1(6):1125–1142.
29. Jaspers JE, Kersbergen A, Boon U, et al. Loss of 53BP1 causes PARP inhibitor resistance in Brca1-mutated mouse mammary tumors. *Cancer Discov*. 2013;3(1):68–81.
30. Sato K, Kitajima Y, Koga Y, et al. The effect of o6-methylguanine-DNA methyltransferase (MGMT) and mismatch repair gene (hMLH1) status on the sensitivity to alkylating agent 1-(4-amino-2-methyl-5-pyrimidinyl)methyl-3-(2-chloroethyl)-3-nitrosourea(ACNU) in gallbladder carcinoma cells. *Anticancer Res*. 2005;25(6B):4021–4028.
31. de Vree PJ, de Wit E, Yilmaz M, et al. Targeted sequencing by proximity ligation for comprehensive variant detection and local haplotyping. *Nat Biotechnol*. 2014;32(10):1019–1025.
32. Cancer Genome Atlas Research Network. Integrated genomic analyses of ovarian carcinoma. *Nature*. 2011;474(7353):609–615.
33. Patch AM, Christie EL, Etemadmoghadam D, et al. Whole-genome characterization of chemoresistant ovarian cancer. *Nature*. 2015;521(7553):489–494.
34. Keller PJ, Lin AF, Arendt LM, et al. Mapping the cellular and molecular heterogeneity of normal and malignant breast tissues and cultured cell lines. *Breast Cancer Res*. 2010;12(5):R87.
35. Derose YS, Wang G, Lin YC, et al. Tumor grafts derived from women with breast cancer authentically reflect tumor pathology, growth, metastasis and disease outcomes. *Nat Med*. 2011;17(11):1514–1520.
36. Zhang X, Claerhout S, Prat A, et al. A renewable tissue resource of phenotypically stable, biologically and ethnically diverse, patient-derived human breast cancer xenograft models. *Cancer Res*. 2013;73(15):4885–4897.
37. Sharma P, Stecklein SR, Kimler BF, et al. The prognostic value of promoter methylation in early stage triple negative breast cancer. *J Cancer Ther Res*. 2014;3(2):1–11.
38. Xu Y, Diao L, Chen Y, et al. Promoter methylation of BRCA1 in triple-negative breast cancer predicts sensitivity to adjuvant chemotherapy. *Ann Oncol*. 2013;24(6):1498–505.
39. Cai F, Ge I, Wang M, et al. Pyrosequencing analysis of BRCA1 methylation level in breast cancer cells. *Tumour Biol*. 2014;35(4):3839–3844.
40. Wang YQ, Zhang JR, Li SD, et al. Aberrant methylation of breast and ovarian cancer susceptibility gene 1 in chemosensitive human ovarian cancer cells does not involve the phosphatidylinositol 3′-kinase-Akt pathway. *Cancer Sci*. 2010;101(7):1618–1623.
41. Mickley LA, Spengler BA, Knutsen TA, et al. Gene rearrangement: a novel mechanism for MDR-1 gene activation. *J Clin Invest*. 1997;99(8):1947–1957.
42. Gu W, Zhang F, Lupski JR. Mechanisms for human genomic rearrangements. *Pathogenetics*. 2008;1(1):4.
43. Bunting SF, Nussenzweig A. End-joining, translocations and cancer. *Nat Rev Cancer*. 2013;13(7):443–454.
44. Diaz LA Jr, Williams RT, Wu J, et al. The molecular evolution of acquired resistance to targeted EGFR blockade in colorectal cancers. *Nature*. 2012;486(7404):537–540.